Solution structure and p43 binding of the p38 leucine zipper motif: coiled-coil interactions mediate the association between p38 and p43

Hee-Chul Ahn, Sunghoon Kim, Bong-Jin Lee*

Research Institute of Pharmaceutical Sciences, College of Pharmacy, Seoul National University, Seoul 151-742, South Korea

Abstract **p38, which has been suggested to be a scaffold protein for the assembly of a macromolecular tRNA synthetase complex, contains a leucine zipper-like motif. To understand the importance of the leucine zipper-like motif of p38 (p38LZ) in macromolecular assembly, the p38LZ solution structure was investigated by circular dichroism and nuclear magnetic resonance spectroscopy. The solution structure of p38LZ showed an amphipathic α-helical structure and characteristics similar to a coiled-coil motif. The protein–protein interaction mediated by p38LZ was examined by an in vitro binding assay. The p43 protein, another non-synthetase component of the complex, could bind to p38LZ via its N-terminal domain, which is also predicted to have a potential coiled-coil motif. Thus, we propose that the p38–p43 complex would be formed by coiled-coil interactions, and the formation of the binary complex would facilitate the macromolecular assembly of aminoacyl-tRNA synthetases.**
© 2003 Published by Elsevier Science B.V. on behalf of the Federation of European Biochemical Societies.

Key words: Coiled-coil motif; Nuclear magnetic resonance; Macromolecular tRNA synthetase complex; Protein–protein interaction

1. Introduction

Aminoacyl-tRNA synthetase (ARS) catalyzes the attachment of an amino acid to its cognate tRNA. ARSs share a highly conserved catalytic domain from bacteria to mammals in the respective synthetases. However, the higher eukaryotic synthetases exhibit distinctive features. Unique hydrophobic peptide appendices are present in the mammalian ARSs, but not in the prokaryotic synthetases [1–5]. Eight synthetase polypeptides with nine ARS functions are present in the multi-ARS complex, which consists of DRS, the bifunctional EPRS, IRS, KRS, LRS, MRS, QRS, and RRS [6–10]. In addition, three non-synthetase components, with molecular masses of 18, 38, and 43 kDa (p18, p38, and p43, respectively), were also isolated from the complex [11–13]. Because of their hydrophobic nature, the unique peptide appendices from the eight synthetase polypeptides were suggested to form the interface for the protein–protein interactions [7–9].

To understand the structural organization and the interactions between the synthetase components of the complex, biochemical and genetic approaches have been employed. The overall structural organization of the complex was revealed to have an elongated U-shape by electron microscopy [10,14]. The protein–protein interactions between the synthetase components of the complex were determined by chemical crosslinking methods [15,16] or by genetic approaches [13].

The non-synthetase components of the macromolecular ARS complex have been attracting attention recently. One of the non-synthetase components, p38, was suggested to be a scaffold of macromolecular assembly [13,17,18]. The p38 protein shares the putative leucine zipper motif [13], and has been proposed to interact with several components of the complex [13,17]. DRS and KRS were each found to bind tightly to p38, while the binding of RRS or QRS to p38 was much weaker [17]. Additionally, p38 is known to be essential for the assembly and the stability of the macromolecular ARS complex in vivo, and deletion analyses of p38 have mapped the organization of the component proteins within the complex [18]. Another non-synthetase component, p43, also plays a role in the macromolecular assembly. The p43 protein is located in the middle of the complex [19], and has also been found to bind to QRS and RRS [17,20]. The sub-complex containing p38, p43, RRS, and QRS was reconstituted in vitro, and it has been proposed that the assembly of the sub-complex proceeds through the binary complex p38–p43, followed by association with RRS and finally with QRS [17].

In this work, to gain insight into the formation of the multi-ARS complex, we focused on the structure and binding specificity of the leucine zipper-like motif of p38 (p38LZ). The structural characterization of p38LZ was accomplished by circular dichroism (CD) and nuclear magnetic resonance (NMR) spectroscopy. The solution structure of the putative leucine zipper motif of p38 was determined, and the binding of p38LZ to other components of the complex was examined in vitro. These results show that the leucine zipper motif of p38 is sufficient to bind to the N-terminal domain of p43, and the association of p38 with p43 is mediated by coiled-coil interactions.

---

*Corresponding author. Fax: (82)-2-872 3632.
E-mail address: lbj@nmr.snu.ac.kr (B.-J. Lee).

2. Materials and methods

2.1. Peptide synthesis

The synthetic peptide $^+H_3$N-SLQALESRQDDILKRLYEL-KAAVDGLSKMI-COO$^-$, p38LZ, corresponding to residues 51–80 of human p38, was purchased from Chiron, Australia. The synthetic peptide was purified by reverse-phase high performance liquid chromatography. The molecular weight of p38LZ, 3405.4 Da, was identified by ion spray mass spectroscopy and was consistent with the theoretical molecular weight of the peptide, 3405.5 Da.

2.2. CD experiments

CD spectra were recorded on a Jasco J-715 CD spectropolarimeter, at 25°C in 2-mm cells from 250 to 190 nm with a scan speed of 20 nm/min, using 50 μM p38LZ. The CD experiments were performed in water, or in 30% or 50% 2,2,2-trifluoroethanol (TFE)/water solutions at pH 4, to inspect the conformation of p38LZ in an aqueous solution or in hydrophobic environments. All spectra were measured three times, and after averaging, the solvent (water or TFE/water solution) signal was subtracted. The degrees of the signal were converted to mean residue molar ellipticity [θ] (deg cm^2/dmol).

2.3. NMR experiments

NMR spectra were obtained on Bruker DRX 500 and 600 MHz spectrometers at 30°C using 3 mM p38LZ. The spectra showed overlapped or degenerated signals in an aqueous buffer solution, at pH 6.5 (data not shown). However, the increase of the TFE-d_3 concentration and the decrease of the pH of the sample to 4.0 eliminated the overlap of the peaks and a narrower line width was acquired. Thus, all NMR measurements for structural calculations were performed in TFE-d_3/water (1:1), pH 4.0, with a peptide concentration of 3 mM. Two-dimensional nuclear Overhauser effect spectroscopy (2D-NOESY) (mixing times of 120 and 200 ms), total correlation spectroscopy (TOCSY) (mixing times of 40 and 60 ms), and double quantum filtered correlation spectroscopy (DQF-COSY) spectra were acquired using presaturation of the H$_2$O resonance by continuous irradiation with a time domain of 2048 (F2)×512 (F1). The sweep widths in both dimensions were 6009.6 Hz for the Bruker DRX 600 spectrometer. The data were processed using NMRPipe [21] and were analyzed using NMRView [22]. The spin systems were identified from the TOCSY and DQF-COSY spectra, and the sequence assignment was unambiguously accomplished using the NOESY spectra (120 ms and 200 ms) by the conventional method [23].

2.4. Structural calculation

Distance restraints were obtained from the NOESY spectrum with a 200 ms mixing time. The volume of the unambiguously assigned NOE cross-peaks was converted to the upper bound distance restraints of 3.0, 4.0, and 5.0 Å (strong, medium, and weak, respectively) and the lower bound distance restraints were taken as the sum of the van der Waals radii of 1.8 Å. As no stereospecific assignment could be made for the methyl and methylene protons, pseudoatom corrections were applied [23]. The ϕ angles were constrained to $-65 \pm 35°$ for the backbone amides, with $^3J_{HNH\alpha} < 6$ Hz from the DQF-COSY experiments. Hydrogen bond restraints were incorporated on the basis of the slowly exchanging amide protons and the characteristic NOE pattern of an α-helix. A total of 303 distance restraints, including 18 hydrogen bond restraints and 15 dihedral angle restraints, were incorporated into the structural calculation using the simulated annealing and energy minimization protocols in the program X-PLOR 3.581 [24].

2.5. In vitro binding assay

The plasmids harboring the full-length, the N-terminal domain (1–147) and the C-terminal domain (148–312) of p43, and the N-terminal appendices of RRS and QRS were prepared as described previously [25]. The corresponding proteins, p43, p43-N, p43-C, RRS-N$^{1-72}$, and QRS-N$^{1-236}$, respectively, were expressed as 6-His-tagged proteins to facilitate their purification and manipulation.

The proteins were purified with Chelating Sepharose (Pharmacia, Uppsala, Sweden), and were dialyzed against binding buffer (20 mM sodium phosphate dibasic, 500 mM NaCl, pH 7.2). Aliquots of the proteins were mixed with the Chelating Sepharose beads. After incubation at 30°C for 30 min, aliquots of p38LZ were added to the protein-bound Chelating Sepharose beads. The concentrations of the

proteins were about 25 μM and that of p38LZ was about 50 μM. The mixtures were incubated for 30 min at 37°C and then centrifuged. The supernatants were discarded and the beads were washed three times with binding buffer. The proteins were eluted from the beads with binding buffer containing 500 mM imidazole. The eluted proteins were subjected to Tris-Tricine sodium dodecyl sulfate–polyacrylamide gel electrophoresis (SDS–PAGE), which achieves enhanced resolution for the smaller proteins or peptides [26]. The protein-bound p38LZ was detected by Coomassie blue staining.

3. Results and discussion

3.1. Sequence comparison of p38LZ with the leucine zipper motif of the yeast transcription factor, GCN4

A putative leucine zipper motif is thought to be located between residues L55 and I80 of the p38 protein [13]. In this experiment, we selected the peptide sequence between S51 and I80 of p38. Fig. 1A shows the schematic structure and the sequence of the leucine zipper-like motif of p38. The peptide sequence between S51 and I80 of p38 was compared with that of the leucine zipper dimerization domain from the yeast transcription factor, GCN4 (GCN4LZ) [27]. The comparison of the two sequences revealed high sequence similarity. The hydrophobic residues were located at the a and d positions in the respective heptad repeats, and even in the remaining regions, moderate sequence homology existed between the two peptide motifs. As shown in Fig. 1B, the helical wheel diagrams of p38LZ and GCN4LZ displayed a similar distribution of hydrophobic residues, suggesting the presence of a leucine zipper motif in p38.

3.2. CD spectra of p38LZ

The structural properties of p38LZ were characterized by CD spectroscopy. In aqueous, 30% and 50% TFE/water solutions, the CD spectra of p38LZ displayed minima near 208 and 222 nm, suggesting that p38LZ adopts an α-helical conformation (Fig. 2). It should be noted that p38LZ has an α-helical structure, even in an aqueous solution. Synthetic peptides preferably adopt random coil structures in an aqueous solution, and their structural transition from coil to helix occurs in TFE/water mixtures [28,29]. However, in our experiments, p38LZ in the aqueous buffer showed a typical α-helical structure, which suggests that the helical structure of p38LZ in the hydrophobic environment was not induced by the addition of TFE. The increase in the CD intensity upon the addition of TFE suggests that the helical content of p38LZ

Table 1
Structural statistics for the ensemble of 20 structures calculated for p38LZ

X-PLOR energies (kcal/mol)	
E_{total}	32.6 ± 0.5
E_{bond}	0.44 ± 0.03
E_{angles}	26.2 ± 0.2
$E_{impropers}$	4.4 ± 0.06
E_{vdw}	0.94 ± 0.38
E_{NOE}	0.59 ± 0.14
Rmsd from idealized geometry	
bonds (Å)	0.001 ± 0.000
bond angles (°)	0.44 ± 0.002
improper torsions (°)	0.35 ± 0.003
Rmsd from experimental restraints	
distances (Å)	0.006 ± 0.001
Rmsd from the mean structure for the backbone/all atoms (Å)	
helical region (L55–L76)	0.51/1.23

A

1   51   80   312

a   d   a   d   a   d   a   d   a

51 S L Q A L E S R Q D D I L K R L Y E L K A A V D G L S K M I 80   : p38 LZ

249 R M K Q L E D K V E E L L S K N Y H L E N E V A R L K K L V 278   : GCN4LZ

B

p38LZ helical wheel:
M79, A72, R65, G75, E68, D61, A54, R58, L76, L69, I62, L55, K78, A71, K64, S57, Q59, L52, Q53, E56, L66, D60, Y67, L63, V73, D74, K70, I80, S77

positions: c, g, f, a, b, e, d

GCN4LZ helical wheel:
L277, E270, K263, R273, H266, E259, Q252, K256, L274, L267, L260, L253, K276, N269, S262, D255, M250, V257, K251, E254, N264, E258, L261, V271, Y265, E268, V278, A272, K275
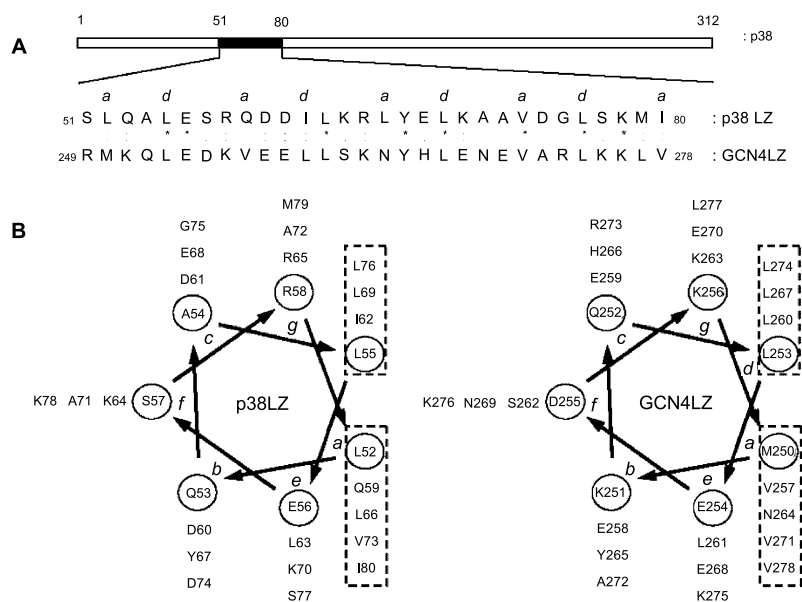
Fig. 1. Sequence comparison of p38LZ with the leucine zipper motif of the yeast transcription factor, GCN4. A: The primary structure of the leucine zipper motif of p38LZ shares sequence homology with GCN4LZ. In each heptad repeat, the *a* and *d* positions are indicated. B: Helical wheel diagrams of p38LZ and GCN4LZ. The residues are indicated by the one-letter amino acid code and the sequence number.

is increased. The isodichroic point at 203 nm indicates that the structures of p38LZ under the three different solution conditions are similar to each other. Thus, it is likely that the structure of the synthetic peptide, p38LZ, reflects the intact structure of this motif in the native p38 protein, and that the putative leucine zipper motif of p38 would intrinsically adopt an α-helical conformation.

3.3. Sequence assignments and secondary structure of p38LZ

The NMR spectrum for p38LZ in an aqueous solution at pH 6.5 showed broad line widths and overlapping of the signals. The broadened line width seems to have originated from the abnormal aggregation of p38LZ, due to its high concentration for the NMR measurements (3 mM p38LZ). The ultracentrifugation experiments to assess the oligomeric state of p38LZ at neutral pH revealed that no dimerization or oligomerization of the peptide had occurred (data not shown). In
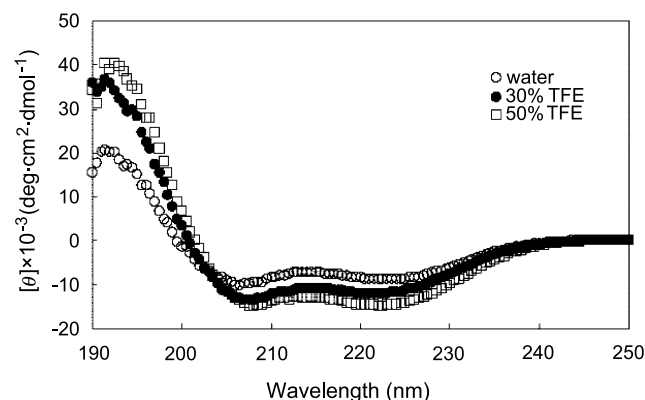
Fig. 2. CD spectra of p38LZ in water (open circles), in 30% (filled circles), and in the 50% TFE/water (open rectangles) solution, at pH 4.0. p38LZ displays an α-helical conformation in the aqueous solution. The addition of TFE increased the intensity of the CD signal and strengthened the stability of the helical p38LZ.

the 50% TFE solution, we obtained a well-dispersed and non-overlapped NMR spectrum. Since p38LZ was proved to have similar structures in the aqueous and TFE/water solutions, we performed all the NMR experiments in the 50% TFE/water solution, at pH 4.0.

Sequence assignments were accomplished from L52 to I80 of p38LZ, from the NOESY spectra. The sequential NOE connectivities are shown in Fig. 3. The presence of the $HN_{(i)}-HN_{(i+1)}$, $H\alpha_{(i)}-HN_{(i+1)}$, $H\alpha_{(i)}-HN_{(i+3)}$, $H\alpha_{(i)}-H\beta_{(i+3)}$, and $H\alpha_{(i)}-HN_{(i+4)}$ NOEs suggests that p38LZ is fully α-helical. Five NOEs between $H\alpha_{(i)}$ and $HN_{(i+2)}$, which often indicate the presence of 3_{10} helices, were found at the N-terminus and in the middle of p38LZ. However, the weak $H\alpha_{(i)}-HN_{(i+2)}$ NOEs are usually found in an α-helix with an average distance of 4.4 Å, as compared to that of a 3_{10} helix, 3.8 Å [23]. Additionally, the helical structure of p38LZ was not broken before and after the regions showing the $H\alpha_{(i)}-HN_{(i+2)}$ NOEs, since $H\alpha_{(i)}-HN_{(i+4)}$ NOEs, which should not be found in the 3_{10} helix [23], appeared consecutively from A54 to K78. Therefore, the authors excluded the possibility of the existence of 3_{10} helices in p38LZ, and concluded that p38LZ adopts a fully α-helical conformation. The measured coupling constant values, $^3J_{HNH\alpha}$, from the DQF-COSY spectrum also support the existence of an α-helix. Furthermore, in the central region of the peptide, the amide protons were slowly exchanged, suggesting that hydrogen bonds are formed and stabilize the helical conformation. The NOE-based secondary structure of p38LZ was consistent with the results of the CD measurement.

3.4. Three-dimensional structure of p38LZ

The three-dimensional structure of p38LZ is shown in Fig. 4, and the structural statistics are shown in Table 1. The p38LZ structure is composed of one well-defined α-helix, spanning the residues from L52 to L76. The N-terminal capping of the helix was inferred, from the $H\alpha_{(i)}-HN_{(i+2)}$ NOE between L52 and A54, to stabilize the helical conformation of
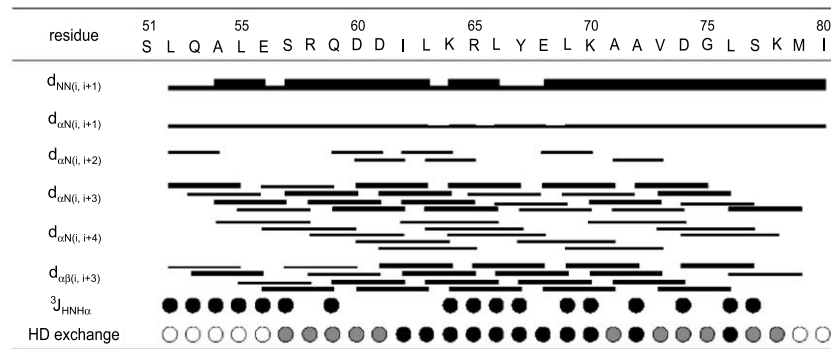
Fig. 3. Overview of the NOE connectivities, coupling constants, and amide proton exchange rates of p38LZ in the 50% TFE/water solution. The thickness of the bar reflects the NOE intensities, which are classified into three groups. The small (< 6 Hz) coupling constants are represented as filled circles. The exchange rates of the amide protons are represented as black (slow), gray (moderate), and white (fast) circles.

p38LZ. The backbone root mean square deviation (rmsd) for the average structure was 0.51 Å for residues L55–L76. The p38LZ structure exhibits typical amphipathic characteristics. One side of the helical region is mainly composed of hydrophobic amino acids, while the hydrophilic amino acids are located on the other side of the helix.

As mentioned previously, p38LZ and GCN4LZ share a similar sequence. The residues at the *a* and *d* positions in each heptad repeat are mainly occupied by hydrophobic amino acids in both motifs. The exceptions are the presence of hydrophilic amino acids, Q59 of p38LZ and N264 of GCN4LZ. Q59 of p38LZ is located at the *a* position in the second heptad repeat, while N264 of GCN4LZ is located at the *a* position of the third repeat. The different positioning of the hydrophilic residues on the hydrophobic side of the amphipathic helix seems to be involved in the binding specificity of the leucine zipper-mediated homo- or heterodimerization.

3.5. In vitro binding of p38LZ with other components of the ARS complex

Previous studies using the yeast two-hybrid method and the deletion mutants of p38 revealed that p38 binds to p43, RRS, and QRS [13,18] and that the amino acids 1–83 of p38 are responsible for the binding to p43 [18]. In our experiments,
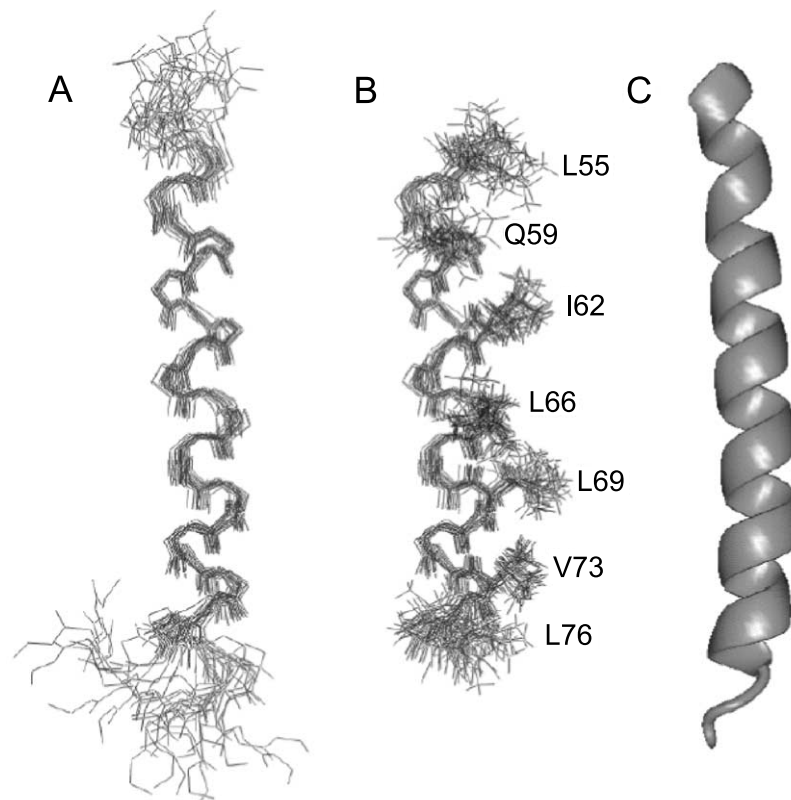

Fig. 4. Solution structure of p38LZ. A: Superimposition of the ensemble of the final 20 simulated annealing structures of p38LZ. B: The central region (L55–L76) of the amphipathic helix, with the side chains at the *a* and *d* positions in each heptad repeat shown. Hydrophobic amino acids are found along one side of the helix. C: Ribbon representation of the average structure of p38LZ. The images were generated by Midas-Plus [36].
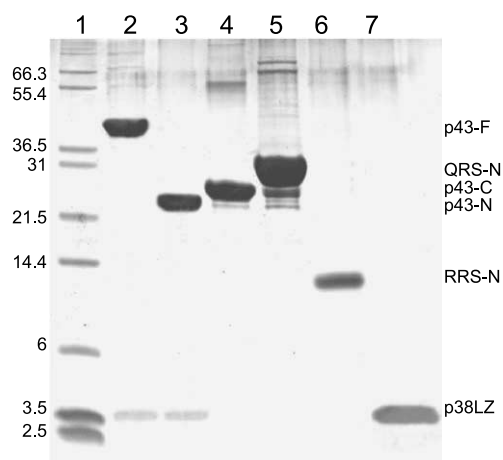
Fig. 5. In vitro binding of p38LZ to other components of the multi-ARS complex. The binding of proteins to p38LZ was confirmed by co-purification of the complex, which was detected by Tris-Tricine SDS–PAGE. Lane 1: molecular weight markers; lane 2: p38LZ-bound p43; lane 3: N-terminal domain of p43. The C-terminal domain of p43 (lane 4), and the N-terminal domains of QRS (lane 5) and RRS (lane 6) could not bind to p38LZ. Lane 7: free p38LZ. Molecular weights are indicated on the left of the figure, and the proteins and peptides are indicated on the right of the figure.

the in vitro binding of p38LZ with other components of the multi-ARS complex was examined. The p43 protein and the hydrophobic polypeptide appendices of RRS and QRS were selected to test the binding to p38LZ, since these appendices were suggested to be the interfaces of the protein–protein interaction [7–9]. As shown in Fig. 5, p43 could bind to p38LZ, while RRS-N$^{1-72}$ and QRS-N$^{1-236}$ could not. To identify the p38LZ binding site of p43, we separately expressed the N-terminal and C-terminal domains of p43 and examined their binding to p38LZ. The leucine zipper motif of p38 was found to bind to the N-terminal domain of p43.

Although we could not quantitatively characterize the binding between p38LZ and p43, the binding seems to be a specific interaction. The in vitro binding of p38LZ to p43 was performed in the presence of the high NaCl concentration (500 mM). Thus, this binding is likely to be strong and specific, which is consistent with the previous result that the binding between p38 and p43 is a strong interaction.

The prediction of coiled-coil motifs by the programs COIL [30] and Paircoil [31] indicated that not only p38, but also p43, RRS, and QRS have a potential coiled-coil motif in their N-terminal domains (Fig. 6). These predicted coiled-coil motifs consist of about 30 amino acids, and p43 and RRS were
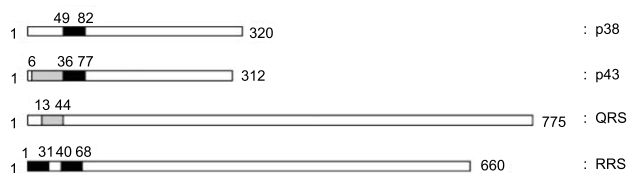

Fig. 6. Prediction of the presence of a coiled-coil motif. The prediction of a coiled-coil motif was performed using the COIL [30] and Paircoil [31] programs. The threshold score of the prediction was 0.5 for both programs. The predicted coiled-coil motifs from both the COIL and Paircoil programs are indicated by black boxes with the residue numbers, and the motifs predicted only by the COIL program are indicated by gray boxes with the residue numbers.

found to have two coiled-coil motifs in their N-terminal domains. However, the in vitro binding experiments showed that only the N-terminal domain of p43 could bind to p38LZ. It has been suggested that discrete interaction sites exist on p38 for each of its interacting partners [13,17], and that there is no competitive binding to p38 between other components [17]. Thus, the binding of p38 to p43 would be responsible for the specific interaction in the coiled-coil manner between the leucine zipper motif of p38 and one coiled-coil motif of p43.

3.6. Implications of the protein–protein interactions

Coiled-coil motifs have been shown to be important for mediating protein oligomerization [32]. These motifs share a characteristic seven-amino acid repeat, $(abcdefg)_n$, with hydrophobic residues at the a and d positions and polar residues generally elsewhere [33–35]. The coiled-coil sequences with this heptad repeat pattern can adopt homo- or heterodimeric conformations. A leucine zipper dimerization domain from the yeast transcription factor GCN4 forms a parallel, dimeric coiled-coil [27]. The p38 protein is known to form a homodimer; however, the dimerization of p38 was shown to occur via the interaction of its C-terminal domain [13]. In this work, the putative leucine zipper motif of p38 showed no evidence of homodimerization in the NMR spectrum and in the ultracentrifugation experiments.

The p38 and p43 proteins are located in the central region of the multi-ARS complex [17,18], and can each bind to several ARSs. Previous studies have indicated that the binding of p38 to p43, DRS or KRS is a strong interaction, and that of p38 to RRS or QRS is weaker [17]. The reconstitution of the sub-complex containing p38, p43, QRS, and RRS revealed that synergistic effects for the association of the weakly interacting proteins are involved in the formation of the macromolecular assembly, and that the formation of the p38–p43 complex is a prerequisite for the subsequent assembly of RRS and QRS [17]. On the basis of deletion analyses of p38 and other previous work, the components of the complex have been grouped into two sub-complexes by their association with p38 [18]. One sub-complex consists of p43, RRS, and QRS anchored to the N-terminal domain of p38. The other sub-complex appeared to be directly or indirectly associated with the C-terminal 236-aa peptide of p38. Based upon our findings, we propose that the association of p38 and p43 should be attributed to the specific coiled-coil interaction. Another coiled-coil interaction is likely to be involved in the protein–protein interaction for the assembly of the multi-ARS complex. The N-terminal domain of RRS was found to bind to the N-terminal domain of p43, where the coiled-coil motifs in RRS and p43 suggested the strong possibility of the involvement of a coiled-coil interaction between the N-terminal domains of the two proteins. Thus, the presence of the coiled-coil motifs in various components of the complex suggests that the coiled-coil-mediated, specific protein–protein interactions are largely involved in the self-association or hetero-oligomerization of the components. These protein–protein interactions between p38, p43, RRS, and QRS would stabilize the complex and contribute to the completion of the assembly of the multi-ARS complex.

4. Concluding remark

A leucine zipper-like motif in p38 was identified, and the

solution structure of this motif was investigated by CD and NMR spectroscopy. The leucine zipper motif of p38 was found to be a single amphipathic α-helix, and its structure was expected to resemble the intact structure in p38. The binding of p38 to p43 was investigated in vitro. The association between p38 and p43 would be formed through the interaction between the leucine zipper-like motif of p38 and the N-terminal domain of p43, and this interaction might occur in a specific coiled-coil manner. The p38–p43 complex is capable of binding with other ARSs to form a multi-ARS complex. Thus, the coiled-coil-mediated p38–p43 complex would provide the scaffold of the protein–protein interactions to stabilize the complex and facilitate macromolecular assembly.

References

[1] Deutscher, M.P. (1984) J. Cell Biol. 99, 373–377.
[2] Mirande, M. (1991) Prog. Nucleic Acid Res. Mol. Biol. 40, 95–142.
[3] Kisselev, L.L. and Wolfson, A.D. (1994) Prog. Nucleic Acid Res. Mol. Biol. 48, 83–142.
[4] Yang, D.C.H. (1996) Curr. Top. Cell. Regul. 34, 101–136.
[5] Ibba, M. and Soll, D. (2000) Annu. Rev. Biochem. 69, 617–650.
[6] Mirande, M., Kellermann, O. and Waller, J.P. (1982) J. Biol. Chem. 257, 11049–11055.
[7] Mirande, M., Le Corre, D. and Waller, J.-P. (1985) Eur. J. Biochem. 147, 281–289.
[8] Cirakoglu, B. and Waller, J.-P. (1985) Eur. J. Biochem. 151, 101–110.
[9] Dang, C.V. and Dang, C.V. (1986) Biochem. J. 239, 249–255.
[10] Norcum, M.T. (1989) J. Biol. Chem. 264, 15043–15051.
[11] Quevillon, S. and Mirande, M. (1996) FEBS Lett. 395, 63–67.
[12] Quevillon, S., Agou, F., Robinson, J.-C. and Mirande, M. (1997) J. Biol. Chem. 272, 32573–32579.
[13] Quevillon, S., Robinson, J.-C., Berthonneau, E., Siatecka, M. and Mirande, M. (1999) J. Mol. Biol. 285, 183–195.
[14] Norcum, M.T. (1999) FEBS Lett. 447, 217–222.
[15] Filonenko, V.V. and Deutscher, M.P. (1994) J. Biol. Chem. 269, 17375–17378.
[16] Norcum, M.T. and Warrington, J.A. (1998) Protein Sci. 7, 79–87.
[17] Robinson, J.-C., Kerjan, P. and Mirande, M. (2000) J. Mol. Biol. 304, 983–994.
[18] Kim, J.Y., Kang, Y.-S., Lee, J.-W., Kim, H.J., Ahn, Y.H., Park, H., Ko, Y.-G. and Kim, S. (2002) Proc. Natl. Acad. Sci. USA 99, 7912–7916.
[19] Norcum, M.T. and Warrington, J.A. (2000) J. Biol. Chem. 275, 17921–17924.
[20] Park, S.G., Jung, K.H., Lee, J.S., Jo, Y.J., Motegi, H., Kim, S. and Shiba, K. (1999) J. Biol. Chem. 274, 16673–16676.
[21] Delaglio, F., Grzesiek, S., Vuister, G.W., Zhu, G., Pfeifer, J. and Bax, A. (1995) J. Biomol. NMR 6, 277–293.
[22] Johnson, B.A. and Blevins, R.A. (1994) J. Biomol. NMR 4, 603–614.
[23] Wüthrich, K. (1986) NMR of Protein and Nucleic Acids, Wiley, New York.
[24] Brünger, A.T. (1992) XPLOR 3.1. A System for X-Ray Crystallography and NMR. Yale University Press, New Haven, CT.
[25] Kim, T., Park, S.G., Kim, J.E., Seol, W., Ko, Y.-G. and Kim, S. (2000) J. Biol. Chem. 275, 21768–21772.
[26] Schagger, H. and von Jagow, G. (1987) Anal. Biochem. 166, 368–379.
[27] O'Shea, E.K., Klemm, J.D., Kim, P.S. and Alber, T.A. (1991) Science 254, 539–544.
[28] Park, S., Park, S.-H., Ahn, H.-C., Kim, S.-K., Kim, S.S., Lee, B.J. and Lee, B.-J. (2001) FEBS Lett. 507, 95–100.
[29] Yoon, M.-K., Park, S.-H., Won, H.-S., Na, D.-S. and Lee, B.-J. (2000) FEBS Lett. 484, 241–245.
[30] Lupas, A., Van Dyke, M. and Stock, J. (1991) Science 252, 1162–1164.
[31] Berger, B., Wilson, D.B., Wolf, E., Tonchev, T., Milla, M. and Kim, P.S. (1995) Proc. Natl. Acad. Sci. USA 92, 8259–8263.
[32] Cohen, C. and Parry, A.D. (1990) Protein 7, 1–15.
[33] Hodges, R.S., Sodek, J., Smillie, L.B. and Jurasek, L. (1972) Cold Spring Harbor Symp. Quant. Biol. 37, 299–310.
[34] McLachlan, A.D. and Stewart, M. (1975) J. Mol. Biol. 98, 293–304.
[35] Conway, J.F. and Parry, D.A. (1990) Int. J. Biol. Macromol. 12, 328–334.
[36] Goodford, P.J. (1985) J. Med. Chem. 28, 849–857.